SUPPLEMENTAL MATERIAL

Gupta et al., https://doi.org/10.1085/jgp.201611673

Phi and r values

We modify and extend phi (Φ) analysis of a linear Markov reaction chain with absorbing end states (C and O) separated by *n* short-lived, intermediate states (T_{1-n}) that we define as the TSE (Zhou et al., 2005):

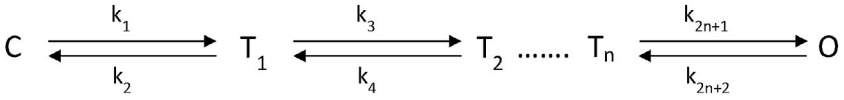

Assuming that the exit rate constants from the end states (k_1 and k_{2n+2}) are much smaller than all of the other rate constants, the mean first passage rate for a complete C→O transition (k_f) is

$$k_f = \frac{k_1}{1 + \sum_{i=1}^{n} \prod_{j=1}^{i} r_j}, \tag{S1}$$

where r_j is the ratio of the exit rates (backward/forward) from T_j. Defining the denominator as M, the Φ values of the reaction chain (first derivative of the rate-equilibrium free energy relationships) are

$$\Phi_q = \frac{\sum_{i=q}^{n} \prod_{j=1}^{i} r_j}{M}. \tag{S2}$$

Note that this corrects Eq. 16 in Zhou et al. (2005).

There are five phi populations for diliganded AChR gating, so $n = 4$ and

$$\begin{aligned}
\Phi_1 &= \frac{(r_1 + r_1 r_2 + r_1 r_2 r_3 + r_1 r_2 r_3 r_4)}{M} \\
\Phi_2 &= \frac{(r_1 r_2 + r_1 r_2 r_3 + r_1 r_2 r_3 r_4)}{M} \\
\Phi_3 &= \frac{(r_1 r_2 r_3 + r_1 r_2 r_3 r_4)}{M} \\
\Phi_4 &= \frac{(r_1 r_2 r_3 r_4)}{M}.
\end{aligned} \tag{S3}$$

$\Phi_5 = 0$, by definition. An example WT energy landscape is the solid line and for a Φ_2 perturbation is the dashed line:

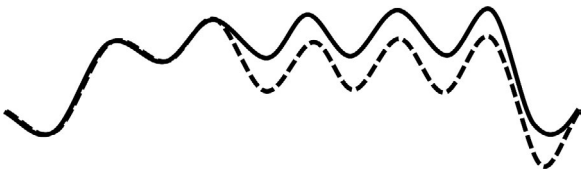

The r values can be calculated from the phi values by solving simultaneous equations represented by a matrix equation: $AY = B$. A is an n-by-n square matrix and Y and B are column vectors of length n:

$$\begin{aligned}
A_{ij} &= \begin{cases} \Phi_i, & i < j \\ (1 - \Phi_i), & i \geq j \end{cases} \\
Y_i &= \prod_{j=1}^{i} r_j \\
B_i &= \Phi_i.
\end{aligned} \tag{S4}$$

Y, and hence r_j values, can be obtained by finding the matrix inverse of A ($Y = A^{-1}B$). For $n = 4$, Eq. S4 is

$$\begin{bmatrix} (1-\Phi_1) & (1-\Phi_1) & (1-\Phi_1) & (1-\Phi_1) \\ -\Phi_2 & (1-\Phi_2) & (1-\Phi_2) & (1-\Phi_2) \\ -\Phi_3 & -\Phi_3 & (1-\Phi_3) & (1-\Phi_3) \\ -\Phi_4 & -\Phi_4 & -\Phi_4 & (1-\Phi_4) \end{bmatrix} \begin{bmatrix} Y_1 \\ Y_2 \\ Y_3 \\ Y_4 \end{bmatrix} = \begin{bmatrix} \Phi_1 \\ \Phi_2 \\ \Phi_3 \\ \Phi_4 \end{bmatrix}. \tag{S5}$$

We write explicitly the set of four simultaneous equations:

$$(1-\Phi_1)\,.\,Y_1+(1-\Phi_1)\,.\,Y_2+(1-\Phi_1)\,.\,Y_3+(1-\Phi_1)\,.\,Y_4 = \Phi_1$$
$$-\Phi_2\,.\,Y_1+(1-\Phi_2)\,.\,Y_2+(1-\Phi_2)\,.\,Y_3+(1-\Phi_2)\,.\,Y_4 = \Phi_2$$
$$-\Phi_3\,.\,Y_1-\Phi_3\,.\,Y_2+(1-\Phi_3)\,.\,Y_3+(1-\Phi_3)\,.\,Y_4 = \Phi_3$$
$$-\Phi_4\,.\,Y_1-\Phi_4\,.\,Y_2+-\Phi_4\,.\,Y_3+(1-\Phi_4)\,.\,Y_4 = \Phi_4.$$

Solving these equations for Y_i,

$$Y_1 = r_1;\ Y_2 = r_1 r_2;\ Y_3 = r_1 r_2 r_3;\ Y_4 = r_1 r_2 r_3 r_4.$$

The experimental diliganded AChR gating phi values are $\Phi_1 = 0.95$, $\Phi_2 = 0.79$, $\Phi_3 = 0.58$, and $\Phi_4 = 0.33$ ($\Phi_5 = 0.06$; Fig. 6 A). Solving for Y (MATLAB R2014b; The MathWorks Inc.) and using the experimental k_f value of 2 ms^{-1} when the overall C-to-O equilibrium constant is equal to 1, the solution is $r_1 = 3.20$, $r_2 = 1.32$, $r_3 = 1.19$, and $r_4 = 1.32$. These values yield M = 19.96 and Scheme 3 (rate constants, ms^{-1}).

From the hypothetical energy landscape for unliganded gating (Fig. 6 E), we calculate r values of $r_1 = 3{,}200$, $r_2 = 1.32$, $r_3 = 1.19$, and $r_4 = 1.32$, to yield Scheme 5. From these r values, we calculate (Eq. S3) unliganded phi values of $\Phi_1 = 0.99$, $\Phi_3 = 0.83$, $\Phi_3 = 0.61$, and $\Phi_4 = 0.35$.

Committor

The position in the reaction chain where there is an equal probability of entering rapidly either absorbing end state is called the committor or separatrix (‡). The position of ‡ in the TSE was calculated (by optimization) from the A matrix (Qin et al., 1996) as the position in the Markov chain in which the probabilities of reaching either absorbing state were equal after time t (long compared with sojourns in the TSE and short compared sojourns in the end states; by Chris Nicolai; http://www.qub.buffalo.edu/online/commitor.html). A ‡ position between T states is the relative probability of either flanking state. In Scheme 3 and with all k values = 300 ms^{-1}, the ‡ probabilities were 80% in T_3 and 20% in T_4.

Transmission coefficient

In Eyring theory, a TS is the point intersection of end-state parabolic wells, and a transmission coefficient (κ) corrects the rate constant for TS re-crossings. In Kramers theory, the separating barrier is a parabola and κ is proportional to the product of a diffusion constant and the barrier frequency (width) under the condition of moderate to high friction (Billing and Mikkelsen, 1996). Here, r values (phi values) set the overall barrier shape and κ is the fraction of exits from an end state that reach the committor ‡, which by definition is crossed with a 50% probability.

With absorbing end states, the number of exits from C that result in one complete passage to O is M. The fraction of visits to ‡ is, then, 2/M:

$$\kappa_{C\to O} = 2 \bullet \left(1+\sum_{i=1}^{n}\prod_{j=1}^{i} r_j\right)^{-1}$$
and (S6)
$$\kappa_{O\to C} = 2 \bullet \left(1+\sum_{i=n}^{1}\prod_{j=n}^{i} \frac{1}{r_j}\right)^{-1}.$$

Note that these correct Eqs. 8 and 9 in Zhou et al. (2005). From the r values for diliganded gating Scheme 3, $\kappa_{C\to O} = 0.10$ and $\kappa_{O\to C} = 0.66$, and for unliganded gating Scheme 5, $\kappa_{C\to O} = 1.1E\text{-}4$ and $\kappa_{O\to C} = 0.7$. With regard to the mean number of the exit attempts required for a full crossing (=2/κ), these four values correspond to approximately 20, 3, 18,000, and 3, respectively.

With ACh, the assumption that the exit rate constant from C << than the other rate constants is not valid. Specifically, the exit rate from C (k_1) is likely to be similar to the rate for exiting the TSE (k_{TSE}). Accordingly,

$$\kappa_{C\to O} = 2\,k_f\left(\frac{1}{k_1}+\frac{1}{k_{TSE}}\right). \quad (S7)$$

The mean number the of exit attempts required for a full C→O crossing is the inverse of half this value.

In WT AChRs with two bound ACh, $k_f = 50$ ms^{-1} (−100 mV, 23°C). However, k_1 is not known, and k_{TSE} depends on the absolute values of the rate constants in Scheme 3. In Fig. 6 E, we have assumed $k_1 = 1{,}000$ ms^{-1}, which is close to maximal (Chakrapani and Auerbach, 2005). With k_3, k_5, k_7, and k_9 in Scheme 3 all equal to 300 ms^{-1}, $k_{TSE} \approx 180$ ms^{-1} (the inverse of the longest TSE time constant, 1/5.6 µs; Fig. 6 B), and we calculate using Eq. S7 that $\kappa_{C\to O} = 0.66$. With these assumptions regarding k_1 and k_{TSE}, the mean number of exit attempts from C before achieving a full C→O crossing is $(\kappa_{C\to O}/2)^{-1}$ or ∼3. The O→T_4 rate constant is slow with or without ACh, so the mean number of exit attempts from O before achieving a full O→C crossing is in both cases also ∼3.

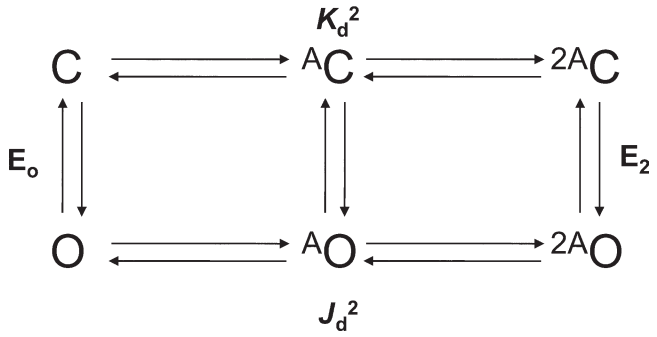

Figure S1. **Cyclic activation model.** C, closed-channel conformation; O, open-channel conformation; superscript A, agonist; K_d, low-affinity equilibrium dissociation constant; J_d, high-affinity equilibrium dissociation constant; E_0, unliganded gating equilibrium constant; E_2, gating equilibrium constant with two bound agonists. Without external energy, the product of equilibrium constants connecting any two states is independent of the pathway (Hess's law). Considering C and ^{2A}O: $(1/K_d^2)\cdot(E_2) = (E_0)\cdot(1/J_d^2)$ or, $E_2/E_0 = (K_d/J_d)^2$.

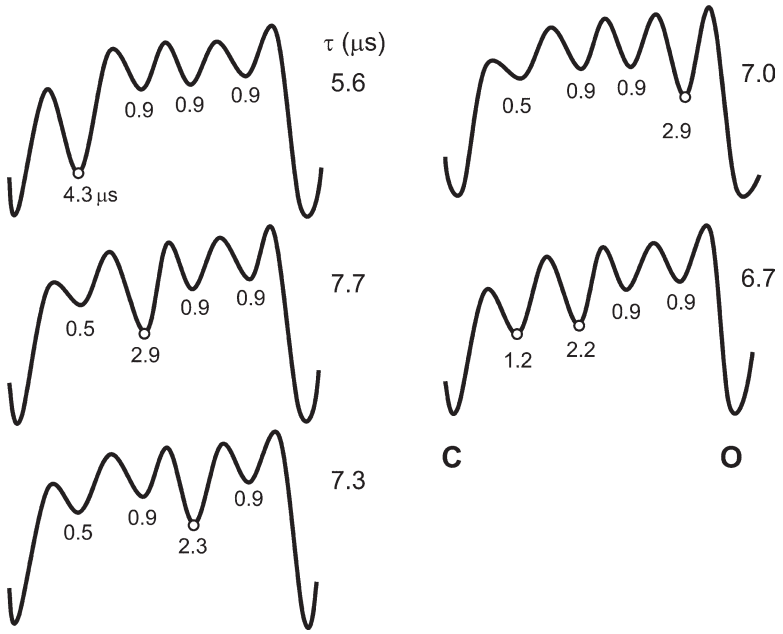

Figure S2. **Energy landscapes corresponding to Scheme 3 with k = 500 ms^{-1}, except for the intermediate state(s) marked by an open circle (Table S3).** τ is the brief shut interval flip/primed lifetime measured after filtering and fitting by C-C′-O (Fig. 6 C). Lifetime (μs) of each TSE intermediate state is shown below each well.

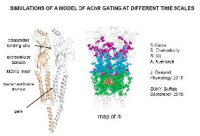

Video 1. **A model of AChR gating.** Part 1 (~2 min): Description of the model detailing the structural components, energy landscape, sequence of rearrangements, and corresponding kinetic scheme. Part 2 (~3 min): Simulations of the model at three different time scales. (top left) Cartoon structure showing components that switch between locally off (black) and on (red) conformations; (top right) gating energy landscape; (bottom) simulated single-channel current. (i) 100 kHz (10 µs/sample). Only sojourns in C and O are clearly resolved. (ii) 2 MHz (500 ns/sample). Sojourns in the T states are also resolved. Notice that C→T structural transitions occur in long-duration shut intervals without a change in current and that brief closures in the current trace (flip/primed events) mainly reflect gate bubble formation. (iii) 50 MHz (20 ns/sample) using two different kinetic models (see Fig. S2).

Table S1. **Backgrounds for MCA analysis**

Mutation(s)	Agonist	Mutant pair
αA96V	100 mM ACh	αS268P+αY190P
αC418W	100 mM ACh	αS268A+αG147A, αP265A+αG147A, αP265A+αW149A, αI260P+αG147A, αI260P+αW149P
αC418Y	100 mM ACh	αP265A+αY198A
	100 mM Cho	αS268A+εP121A, αS268A+εP121S, αS268A+δP123A
αC418W+δI43Q	100 mM ACh	αP265G+αW149P
αC418Y+δI43Q	100 mM ACh	αI260P+αY190P
βT456F	100 mM ACh	αP265A+αY190F, αI260P+δP123G,
βT456F+δI43H	100 mM ACh	αP265A+αY93A, αI260P+εP121G,
βT456I+δI43H	100 mM ACh	αP265A+γP112A
βV229A+δI43Q	100 mM ACh	αS268P+εP121G, αP265G+εP121G
δI43Q	20 mM Cho	αS269A+αT133A, αA270G+αT133A, αS266A+εK219A, αT267A+εK219A
δI43H	100 mM ACh	αE262G+αY93A, αE262G +αW149A, αL263G+αY93A, αL263G+αW149A, αL263G+αY198A
δI43Q+γL260Q	100 mM ACh	αP265A+αG147A(γ)
εL269F	100 mM ACh	αS268P+αW149P
αA96V+β V266A+dP123R	100 mM ACh	γP121A+αY93A
αA96V+ βL262S+δL265S+δP123R	No agonist	γP121A+αG147A
βL262S+δL265S+δP123R	100 mM ACh	γP121A+αG147A, γP121A+αW149A, γP121A+αY190A, γP121A+αY198A, γP121A+γW55A
	No agonist	γP121A+αW149A, γP121A+αY198A
δP123R	100 mM ACh	γP121A+αG153A

Table S2. **Backgrounds for unliganded REFERs (Fig. 5)**

Mutation	Background(s)
αI260M	α(D97A+Y127F+S269I+W149F)
S	α(D97A+Y127F+S269I+W149F)+δV269C
A	α(D97A+Y127F+S269I+W149F+C418W)
αE262G; L	α(D97A+Y127F+S269I+W149F)
αP265K	α(D97A+Y127F+S269I+W149F+C418W)
G	α(D97A+Y127F+S269I)
αS268E	δI43Q
D	α(D97A+Y127F)
L	α(D97A+Y127F)+δV269C

Table S3. **Simulation results using Scheme 3 and different k values**

k	τ^{sim}	τ^{flip}	k_f	k_b
ms^{-1}	μs	μs	ms^{-1}	ms^{-1}
100	15.8	15.2	35	30
200	8.4	9.3	51	55
300	5.6	6.4	61	82
400	4.3	5.8	61	107
500	3.5	5.0	58	137
600	2.9	4.6	49	161

τ^{sim} is the slowest component of the simulated TSE shut distribution (Fig. 6 B), τ^{flip} is the fitted shut component in facsimile patch experiments (Fig. 6 C), k_b and k_f are the fitted exit rate constants from C′, backward and forward. In experiments with human adult AChRs expressed in cells, τ^{flip} ~9 µs, k_f ~19 ms^{-1}, k_b ~86 ms^{-1}.

Table S4. **Effects of stabilizing individual TSE states**

n	λ	τ	k_f	k_b	ΔG	k_{right}
	μs	*μs*	ms^{-1}	ms^{-1}	*kcal/mol*	ms^{-1}
1	5.2	5.6	46	128	1	55
2	6.3	7.7	37	88	0.74	150
3	6.1	7.3	53	80	0.5	200
4	5.9	7.0	79	62	0.7	150
1; 4	5.3	6.7	45	99	0.54	200

λ, τ, k_f, and k_b as in Table S3. ΔG, the free energy by which state(s) n was stabilized. k_{right}, forward exit rate constant from stabilized state(s). Corresponding energy landscapes are shown in Fig. S1.

REFERENCES

Billing, G.D., and K.V. Mikkelsen. 1996. Introduction to Molecular Dynamics and Chemical Kinetics. John Wiley & Sons, Inc., New York. 200 pp.

Chakrapani, S., and A. Auerbach. 2005. A speed limit for conformational change of an allosteric membrane protein. *Proc. Natl. Acad. Sci. USA*. 102:87–92. http://dx.doi.org/10.1073/pnas.0406777102

Qin, F., A. Auerbach, and F. Sachs. 1996. Estimating single-channel kinetic parameters from idealized patch-clamp data containing missed events. *Biophys. J.* 70:264–280. http://dx.doi.org/10.1016/S0006-3495(96)79568-1

Zhou, Y., J.E. Pearson, and A. Auerbach. 2005. Phi-value analysis of a linear, sequential reaction mechanism: theory and application to ion channel gating. *Biophys. J.* 89:3680–3685. http://dx.doi.org/10.1529/biophysj.105.067215